EXTENSION OF THE CAUCASUS SEISMIC INFORMATION NETWORK STUDY INTO CENTRAL ASIA

Randolph Martin[1], Mary L. Krasovec[1], Spring Romer[1], M. Nafi Toksöz[2], and Levent Gülen[2]

New England Research[1] and Massachusetts Institute of Technology[2]

Sponsored by National Nuclear Security Administration
Office of Nonproliferation Research and Development
Office of Defense Nuclear Nonproliferation

Contract Nos. DE-AC-52-04NA25612[1] and NNSA-4-45[2]

ABSTRACT

The Central Asian Seismic Research Initiative (CASRI) is an extension of the Caucasus Seismic Information Network (CauSIN). Both projects seek to build knowledge bases of geological, geophysical, and seismic information in their respective regions and to use crustal modeling techniques to create a combined model of the regions to aid in seismic monitoring.

Tectonically, the most complex region in central Asia is the Tien Shan region. It is an intracontinental convergence region consisting of igneous and metamorphic ranges and major basins. The east-west trending morphology is the result of reactivation of the old structures in the late Cenozoic. Folding, thrusting and high-angle reverse faults are the most dominant forms of deformation.

The crust upper mantle structure of the region, primarily based on global tomography and receiver function analysis, is highly variable. New seismic data from local and regional stations are becoming available. We will use the travel-time data to generate a 3-D Moho map and the associated P_n velocity model for the region.

OBJECTIVES

The primary goal of this project is to develop a database of geology, tectonics, and seismicity for central Asia which covers Kazakhstan, Uzbekistan, Kyrgyzstan, and Tajikistan, basically extending and complimenting the work that we have accomplished for the CauSIN project countries (Georgia, Armenia, Azerbaijan, and northeastern Turkey) in the west (Figure 1).

We will be able to improve the event locations with this new data base which will include data from denser seismic networks that have improved and upgraded instrumentation with broadband seismometers, calibration events (mining and quarry blasts), improved models, and better location algorithms (e.g., double difference, multiple-event grid search etc).

We will obtain 3-D crust/upper mantle structure in the Central Asia using data from local seismic stations as well as other stations operated as part of the national networks. Extensive geological and geophysical data (e.g., surface seismic reflection profiles, gravity maps) as well as seismic data will be utilized in the construction of the lithospheric models.

RESEARCH ACCOMPLISHED

One of the deliverables of the CauSIN and CASRI projects is a geological map compilation covering the Caucasus and the central Asia region. Such a geological map was prepared in Arc geographical information system (GIS) digital format (Figure 2). The geological map of Asia and Europe (1:5,000,000 scale) that was originally compiled by Tingdong et al. (1997) was used, different sheets were merged seamlessly, and the map projection was converted into the Lambert equal-area projection.

Since most of the seismic activity that occurs in the CASRI countries is associated with the Tien Shan, an extensive literature survey was carried out, and this paper summarizes the detailed technical report that was prepared on the active tectonics of the Tien Shan, Central Asia (Gülen and Toksöz, 2006).

Geology and Tectonics of the Tien Shan

The active tectonics of central Asia is a consequence of the continental collision and the continuing continental convergence between the Indian and the Eurasian plates. This continental collision is considered to be the most important geological event of the Cenozoic era because it has created a 2500 km long mountain chain, the Himalayas, that contains the highest elevations on earth, and an immense plateau, Tibet, that has an average elevation of more than 5,000 m and an areal extent of 700,000 km^2. It also tectonically reactivated and uplifted the 2,500-km-long Tien Shan ranges 1,500 km to the north.

The Tien Shan is a prominent mountain belt of central Asia that rises north of the Pamir and the Tarim Basin and extends for 2,500 km from the Kizil Kum in the west to the Gobi Desert in the east (Figure 3). It is bounded by the Kazakh Platform and the Junggar (Dzungarian) Basin in the north. The Tien Shan is composed of E-W trending mountain ranges of mainly Paleozoic rocks that are separated by intermountain basins filled with Mesozoic and Cenozoic sediments, and its width increases towards the west, reaching 400 km at 76°E (Burtman, 1975; Tapponnier and Molnar, 1979; Avouac et al., 1993). A major NW–SE trending, right-lateral strike-slip fault, the Talas-Fergana Fault forms a major discontinuity between the western Tien Shan (Chatkal Ranges) and the central Tien Shan.

The structure of the greater part of the Tien Shan was formed in the Late Paleozoic and it was an active tectonic era of crustal deformation evidenced by widespread folding, trust and strike-slip faulting (Burtman, 1975; Tapponnier and Molnar, 1979; Burtman, 1980). Metamorphosed Carboniferous ophiolites mark the suture of the northward subducting Turkestan Paleozoic ocean along the long axis of the Tien Shan in the north. (Lee et al., 1982; Khain, 1985; Watson et al., 1987; Dewey et al., 1988; Burtman et al., 1996). The Tien Shan basement was fully amalgamated to Eurasia along the Tien Shan Suture Zone by the end of the Paleozoic (Burtman, 1975, Tapponnier and Molnar, 1979; Avouac et al., 1993).

Active Crustal Deformation and Shortening in the Tien Shan

The present E–W trending morphology, high elevation, and structure of the Tien Shan, which contains a number of mountain ranges and intermountain basins squeezed between them, is formed mainly as a result of late Cenozoic tectonics. In general, folding, thrusting, and high angle reverse faulting are by far the most dominant form of deformation in the Tien Shan. The E-W trending, active thrust systems form the northern and southern boundaries of the Tien Shan mountain range (Molnar and Tapponnier, 1975; Tapponnier and Molnar, 1979; Yin et al., 1998). Mostly, the marginal fold and thrust belts of the Tien Shan Ranges have a structural vergence that is toward the flanking basins, such as the Junggar and Tarim basins to the north and south, respectively, but there are well-developed exceptional structures that have an opposite vergence as well (Burchfiel et al., 1999). In fact, thrust faulting extensively defines the boundaries of almost all the mountain ranges and basins within the Tien Shan and along its boundaries (Cobbold et al., 1996; Burbank et al., 1999; Abdrakhmatov et al., 2002; Thompson et al., 2002).

For example Issyk Kul, Suusamyr, Kochkor, Naryn, At-Bashi, and Aksay are such intermontaine basins that are bounded by E–W trending thrust faults at the basin boundaries (Figure 3).

Recent GPS measurements carried out by numerous campaigns through multilateral collaborations provide important data on the rates of crustal shortening in the Tien Shan (Abdrakhmatov et al., 1996; Wang et al., 2001; Reigber et al., 2001) and the rest of Asia. These measurements confirm active shortening rates of about 20 mm yr^{-1} for the Tien Shan. Wang et al. (2001) also measured the India-Eurasia convergence rate by GPS and they obtained 38 mm yr^{-1}, which suggests that the crustal shortening in the central Tien Shan takes up about half of the total convergence between India and Eurasia.

Talas-Fergana Strike-Slip Fault

The Talas-Fergana Fault is a major right-lateral strike slip fault that runs from the northwestern corner of the Tarim Basin, traverses the Tien Shan Ranges for about 500 km in the northwest direction, and extends well into the Kazakh Platform with a total length of over 1500 km (Figure 3; Burtman, 1975; Tapponnier and Molnar, 1979; Burtman, 1980; Burtman et al., 1996). This fault separates the Chatkal Ranges (the NW corner of the Tien Shan), the Fergana Basin, and the Alay Ranges (Tien Shan Range north of the Pamir) from the central Tien Shan and it consists of two major segments. The Talas-Fergana Fault, after crossing the Tien Shan Ranges, makes a right step-over in the north and continues in the Kazakh Platform. This northwestern segment is also referred to as the Karatau Fault (Burtman et al., 1996). On satellite images and high resolution shuttle radar topographic mission (SRTM) images it can be seen clearly that numerous thrust faults of the Tien Shan Ranges, on both sides of the Talas-Fergana strike-slip fault, abruptly terminate along the fault trace indicating that the Talas-Fergana Fault forms a major crustal discontinuity.

The Talas-Fergana Fault originated during the intense tectonic activity occurred in this region in the late Paleozoic time (Burtman, 1975; 1980). The Paleozoic igneous intrusions and tectonic structures have been displaced right-laterally ~ 180 km along the Talas-Fergana Fault and the amount of right-lateral displacement is estimated to be 60 ± 10 km since the early Cretaceous time (Burtman et al., 1996). The lack of seismic activity along this fault during the entire instrumental period is rather interesting and may suggest that The Talas-Fergana fault is presently locked and the present-day activity appears to stem from the active shortening on both sides of the fault (Ghose et al., 1998a,b).

Seismicity of the Tien Shan

The Tien Shan is seismically very active (Figure 4) and this is not surprising, because the entire region is characterized by roughly E-W trending active thrust faults, both along its outer margins, as well as along the numerous intermontane basin margins with the bounding mountain ranges.

One of the important characteristics of the Tien Shan seismicity is its shallow crustal nature. Although, excluding the Pamir region, a few events appear to be deeper than 50 km, there is no clear evidence of earthquakes occurring in the continental mantle lithosphere of the Tien Shan (north of 40°N), and the seismic activity is confined to the continental crust (Chen and Molnar, 1983; Maggi et al., 2000). As pointed out by Maggi et al. (2000), among the events that have well determined centroid depths constrained by teleseismic and regional P and SH body wave modeling, only 10 events occurred at the depth range of 20–44 km, and the majority of them have depths less than 20 km.

The focal mechanism solutions for the earthquakes in the Tien Shan region indicate predominantly thrust events, with roughly E-W trending fault planes, that provide evidence for the overall N-S active crustal shortening of the Tien Shan (Ni, 1978; Tapponnier and Molnar, 1979; Nelson et al., 1987; Ghose et al.,1998a,b).

Another important feature of the Tien Shan seismicity is a general relationship between the geological structure and the earthquake magnitude. For example, in the Gissar-Kokshal area, north of the Tadjik Basin, the low angle frontal thrusts that move over sedimentary rocks are associated with small magnitude earthquakes, while moderate size (M <5.5) earthquakes occur on crustal thrust ramps that have higher dips, and major strain releases (5.5 >M >8.1) occur along the basement thrusts that form the Tien Shan margin (Leith and Simpson, 1986). This general relationship appears to be valid for the Tien Shan and probably for most of the active fold and thrust belts of the world.

During the last 120 years 12 large earthquakes (M ≥7) occurred along the northern and southern margins of the Tien Shan (Chen and Molnar, 1977; Tapponnier and Molnar, 1979; Molnar and Ghose, 2000; Abdrakhmatov et al., 2002). Among these Verny (the old name for Almaty, 1887, M = 7.3), Chilik (1889, M = 8.3), Manas (1906, M = 8.3), Kemin (1911, M = 8.2), Chatkal (1946, M = 7.5), and Suusamyr (1992, M = 7.3) earthquakes occurred along the northern margin. The large earthquakes that occurred along the southern margin are: Kashgar (1902, M = 7.8), Karatagh (1907, double shock with M = 7.3 and 7.4), Khait (1949, M = 7.4), and Wuqia (1985, M = 7.6).

The Lithospheric Structure of the Tien Shan

The lithospheric structure of the Tien Shan is extremely variable and therefore complex starting from the surface, through the crust, to all the way down to the mantle (Figure 5). Since the nineties many studies have been carried out to reveal the lithospheric structure of the Tien Shan (Kosarev et al., 1993; Roecker et al., 1993; Cotton and Avouac, 1994; Ghose et al., 1998a,b; Bump and Sheehan, 1998; Oreshin et al., 2002; Vinnik et al., 2002a,b; Poupinet et al., 2002; Vinnik et al., 2004; Kumar et al., 2005).

The first P receiver function application in the Tien Shan indicated significant crustal velocity differences on both sides of the Talas-Fergana Fault (Koserev et al., 1993). The crustal velocities are 10% higher on the west side of the Talas-Fergana Fault at the 10–35 km depth range and the areas east of the fault are associated with lower mantle velocities, low Q, and shorth-wavelength variations in anisotrophy. These differences were interpreted as due to mantle upwelling, which may have contributed to the vertical uplift of the Tien Shan ranges on the west side of the Talas-Fergana Fault.

P and S wave tomographic study of Roecker et al. (1993) determined that the Chu and Fergana Basins have 7 km and 10 km thick sediments, respectively. The differences on both sides of the Fergana Fault were confirmed (Roecker et al., 1993; Ghose et al., 1998a,b) and they suggested that the 10% lower mantle velocities on the west side of the Talas-Fergana Fault, beneath the central Tien Shan exceed 150 km depth, but no deeper than 300 km.

Surface wave-dispersion, P and S tomography and receiver function studies have produced Moho depth values in the range of 45 to 70 km in the Tien Shan (Roecker et al., 1993; Cotton and Avouac, 1994; Mahdi and Pavlis, 1998; Bump and Sheehan, 1998; Oreshin et al., 2002; Vinnik et al., 2002 & 2004; Kumar et al, 2005). This reported range in Moho depth is real and demonstrates the extremely variable nature of the lithospheric structure in the Tien Shan.

Using simulated annealing technique, Vinnik et al. (2004) inverted P and S receiver functions together for 40 broad-band stations to obtain receiver function tomographic images of the Tien Shan lithosphere. The P and S receiver function tomography indicates that the Moho depth varies between 45 km to about 70 km beneath the Tien Shan. The Kazakh Platform, the Tarim Basin have thinner crust (~45 km), whereas within the Tien Shan Ranges, west of the Lake Issyk-Kul the crustal thickness reaches up to 70 km. The crust is thin (~45 km) beneath the Naryn Basin and the immediate west of the Talas-Fergana Fault. Interestingly, the elevated crustal thickness correlates with a thickened “basaltic” layer (Vs ~ 4.0 km s^{-1}) in the lower crust and the presence of low-velocity zones in the uppermost mantle, suggesting that recent magmatic underplating is also responsible for crustal thickening in addition to the crustal shortening (Vinnik et al., 2004).

The lithosphere and asthenospere boundary (LAB) in the Tien Shan and surrounding regions vary significantly based on another S receiver function study by Kumar et al. (2005). They found that, along a N-S profile at 75°E, the LAB is 130 km deep beneath the Kazakh Platform and 90 km deep beneath the Tien Shan (40°–41°N) confirming the results obtained by Oreshin et al. (2001) and Vinnik et al. (2004). The lithospheric thickness is 180 km in the Tarim Basin and the LAB starts dipping toward south reaching a depth of 270 km beneath Pamir, where it correlates with the intermediate-depth seismicity, which is interpreted as an evidence for the continental subduction of the Asian lithosphere (Kumar et al., 2005). This geometry of the LAB correlates well and forms the upper boundary of a low-velocity anomaly dipping toward south from a depth of 90 km beneath the Tien Shan to 300 km beneath the Karakoram imaged by surface wave tomography (Freiderich, 2003).

Similarly, southward subduction of the Tarim plate with ~ 45° angle, down to ~300 km depth beneath northwestern Tibet has been suggested based on the results obtained from receiver function and P-wave tomography (Wittlinger et al., 2004).

On the other hand, teleseismic receiver function analysis (Poupinet et al., 2002) and seismic refraction/wide-angle-reflection studies (Zhao et al., 2003; 2006) along a northeast trending profile from the Tarim Basin to the Junggar Basin suggest that the Moho at the northern margin of the Tarim basin dips north beneath the Tien Shan. Also the Moho at the southern margin of the Junggar Basin dips south beneath the Tien Shan. The results obtained from a larger scale P-wave tomographic study of the southeast Asia (Li et al., 2006) appear to confirm only the southward subduction of the Junggar lithosphere. However, this does not necessarily rule out the northward subduction of the Tarim lithosphere, because as reported by Li et al. (2006) the resolution of their P-wave tomographic model beneath the Tarim Basin is rather poor. Furthermore, they state that no prominent high velocity is detected beneath the Tarim Basin, which is contradicted by the results obtained from surface wave velocity inversion, receiver function tomography, and P-wave tomography (Villaseñor et al., 2001; Vinnik et al., 2004; Sun and Toksöz, 2006).

CONCLUSIONS AND RECOMMENDATIONS

The current structure of the Tien Shan is formed by the reactivation of Paleozoic structures in the Late Cenozoic due to the India-Asia plate collision. Roughly east-west trending folding, thrusting and high-angle reverse faulting is the dominant form of crustal deformation. The Tien Shan region has high seismic activity, and many large earthquakes that have predominantly thrust faulting mechanisms occurred in the region. Based on the GPS measurements the active crustal shortening rate is 20 mm yr^{-1} in the Tien Shan. This rate corresponds to the half of the total plate convergence between the Indian and Eurasian plates. The lithospheric structure of the Tien Shan is extremely complex, and the Moho depth varies between 45–70 km. The thicker crust correlates with a thickened basaltic layer in the lower crust and the presence of low-velocity zones in the upper-mantle. Seismic tomographic and S-receiver function studies indicate a southward dipping LAB that suggests the southward subduction of the continental lithosphere in the western Tien Shan. The lithospheric mantle beneath the Junggar Basin appears to subduct southward beneath the Tien Shan. Our recommendation for the next step in this research is to integrate tectonic models with the crustal structure which will be determined from new data from local networks in the participating countries.

REFERENCES

Abdrakhmatov, K. Y. et al. (1996). Relatively recent construction of the Tien Shan inferred from GPS measurements of present day crustal deformation rates, *Nature*, 384: 450–453.

Abdrakhmatov, K. Y., K. D. Djanuzakov, and D. Delvaux (2002). Active tectonics and seismic hazards of the Issyk-Kul Basin in the Kyrgyz Tian Shan, in *Lake Issyk-Kul: Its Natural Environment*, J. Klerkx and B. Imanackunov (Eds.).Norwell, Massachusetts: Kluwer Academic Publishers, pp. 147–160.

Avouac, J. P., P. Tapponnier, M. Bai, H. You, and G. Wang (1993). Active thrusting and folding along the northern Tien Shan and Late Cenozoic rotation of the Tarim relative to Dzungaria and Kazakhstan, *J. Geophys. Res*. 98: 6,755–6,804.

Bump, H. A. and A. F. Sheehan (1998) Crustal thickness variations across the northern Tien Shan from teleseismic receiver functions, *Geophys. Res. Lett.* 25: 1,055–1,058.

Burbank D. W., J. K. McLean, M. Bullen, K. Y. Abdrakhmatov, and M. M. Miller (1999). Partitioning of intermontane basins by thrust-related folding, Tien Shan, Kyrgyzistan, *Basin Res.* 11: 75–92.

Burchfiel, B. C., E. T. Brown, Q. Deng, X. Feng, J. Li, P. Molnar, J. Shi, Z. Wu, H. You (1999). Crustal shortening on the margins of the Tien Shan, Xinjiang, China, *Int. Geol. Rev*. 41: 665–700.

Burtman, V. S. (1975). Structural geology of the Variscan Tien Shan, USSR, *Am. J. Sci*. 272-A: 157–186.

Burtman, V. S. (1980). Faults in middle Asia, *Am. J. Sci*. 280: 725–744.

Burtman, V. S., S. F. Skobelev, and P. Molnar (1996). Late Cenozoic slip on the Talas-Ferghana fault, the Tien Shan, central Asia, *Geol. Soc. Am. Bull*. 108: 1,004–1,021.

Chen, W. P. and P. Molnar (1983). Focal depths of intracontinental and intraplate earthquakes and their implications for the thermal and mechanical properties of the lithosphere, *J. Geophys. Res*. 88: 4,183–4,214.

Cobbold, P. R., E. Sadybakasov, and J. C. Thomas (1996). Cenozoic transpression and basin development, Kyrgyz Tien Shan, central Asia, in *Geodynamic Evolution of Sedimentary Basins*, F. Roure, N. Ellouz, V. S. Shein, and I. Skvortsov (Eds.). Paris: Technip, 181–202.

Cotton, F. and J. P. Avouac (1994). Crustal and upper-mantle structure under the Tien Shan from surface-wave dispersion, *Phys. Earth Planet Int*. 84: 95–109.

Dewey, J. F., R. M. Shackleton, C. Chang, and Y. Sun (1988). The tectonic evolution of the Tibetan Plateau, in The Geological Evolution of Tibet C. Chang, R. M. Shackleton, J. F. Dewey, and J. Yin (Eds.). Royal Society of London Philosophical Transactions, pp. 379–413.

Friederich, W. (2003). The S-velocity structure of the east Asian mantle from inversion of shear and surface waveforms, *Geophys. J. Int*. 153: 88–102.

Ghose, S., M. W. Hamburger, and C. J. Ammon (1998a). Source parameters of moderate-sized earthquakes in the Tien Shan, central Asia from regional moment tensor inversion, *Geophys. Res. Lett*. 25: 3,181–3,184.

Ghose, S., M. W. Hamburger, and J. Virieux (1998b). Three-dimensional velocity structure and earthquake locations beneath the northern Tien Shan of Kyrgyzstan, central Asia, *J. Geophys. Res.* 103: 2,725–2,748.

Gülen, L. and M. N. Toksöz (2006). Active Tectonics of the Tien Shan, central Asia, Earth Resources Laboratory, Massachusetts Institute of Technology report, 88 pp.

Khain, V. E. (1985). *Geology of the USSR, First Part: Old Cratons and Paleozoic Fold Belts*. Berlin: Gebrüder Borntraeger, 264 pp.

Kosarev, G. L., N. V. Petersen, and L. P. Vinnik (1993). Receiver functions for the Tien Shan analog broadband network: Contrasts in the evolution of structures across the Talasso-Fergana Fault, *J. Geophys. Res*. 98: 4,437–4,448.

Kumar, P., X. Yuan, R. Kind, and G. L. Kosarev (2005). The lithosphere-asthenosphere boundary in the Tien Shan-Karakoram region from S receiver functions: Evidence for continental subduction, *Geophys. Res. Lett.* 32: L07305, doi: 10.1029/2004GL022291.

Lee, C. Y., Q. Wang, X. Liu, and Y. Tang (1982). Explanatory notes to the tectonic map of Asia, Beijing: Institute of Geology and Geophysics, Chinese Academy of Sciences, 49 pp.

Leith, W. and D. W. Simpson (1986). Seismic domains within the Gissar-Kokshal seismic zone, Soviet central Asia, *J. Geophys. Res*. 91: 689–699.

Li, C., R. D. van der Hilst, and M. N. Toksöz (2006). Constraining P-wave velocity variations in the upper mantle beneath Southeast Asia, *Phys. Earth Planet. Int.* 154: 180–195.

Maggi, A., J. A. Jackson, K. Priestley, and C. Baker (2000). A re-assessment of focal depth distributions in southern Iran, the Tien Shan and northern India: Do earthquakes really occur in the continental mantle? *Geophys. J. Int*. 143: 629–661.

Mahdi, H. and G. L. Pavlis (1998). Velocity variations in the crust and upper mantle beneath the Tien Shan inferred from Rayleigh wave dispersion: Implications for tectonic and dynamic processes, *J. Geophys. Res*. 103: 2,693–2,703.

Molnar, P. and P. Tapponnier (1975). Cenozoic tectonics of Asia, *Science* 189: 419–426.

Molnar, P. and S. Ghose (2000). Seismic moments of major earthquakes and the rate of shortening across the Tien Shan, *Geophys. Res. Lett*. 27: 2,377–2,380.

Nelson, M. R., R. McCaffrey, and P. Molnar (1987). Source parameters for 11 earthquakes in the Tien Shan, central Asia, determined by P and SH waveform inversion, *J. Geophys. Res*. 92: 12,629–12,648.

Ni, J. (1978). Contemporary tectonics in the Tien Shan region, *Earth Planet Sci. Lett*. 41: 347–354.

Oreshin, S., L. P. Vinnik, D. Peregoudov (2002). Lithosphere and asthenosphere of the Tien Shan imaged by S receiver functions, *Geophys. Res. Lett.* 29: 1191, 10.1029/2001GL014441.

Poupinet, G., J. P. Avouac, M. Jiang, S. Wei, E. Kissling, G. Herquel, J. Guilbert, A. Paul, G. Wittlinger, H. Su, and J. C. Thomas (2002). Intracontinental subduction and Paleozoic inheritance of the lithosphere suggested by a teleseismic experiment across the Chinese Tien Shan, *Terra Nova*, 14: 18–24.

Reigber, C., G. W. Michel, R. Galas, D. Angerman, J. Klotz, J. Y. Chen, A. Papschev, R. Arslanov, V. E. Tzurkov, and M. C. Ishanov (2001). New space geodetic constraints on the distribution of deformation in Central Asia, *Earth Planet. Sci. Lett*. 191: 157–165.

Roecker, S. W., T. M. Sabitova, L. P. Vinnik, Y. A. Burmakov, M. I. Golvanov, R. Mamatkanova, and L. Munirova (1993). Three-dimensional elastic wave velocity structure of the western and central Tien Shan, *J. Geophys. Res*. 98: 15,779–15,795.

Sun, Y. and M. N. Toksöz (2006). Crustal structure of China and surrounding regions from P wave traveltime tomography, *J. Geophys. Res*. 111: B03310 doi:10.1029/2005JB003962.

Tapponnier, P. and P. Molnar (1979). Active faulting and Cenozoic tectonics of the Tien Shan, Mongolia, and Baykal regions, *J. Geophys. Res*. 84: 3425–3459.

Thompson, S. C., R. J. Weldon, C. M. Rubin, K. Abrakhmatov, P. Molnar, and G. W. Berger (2002). Late Quaternary slip rates across the central Tien Shan, Kyrgyzstan, central Asia, *J. Geophys. Res*. 107(B9): 2203, doi:10.1029/2001JB000596.

Tingdong, L., et al. (1997). *Geological Map of Asia and Europe* (Scale: 1:5,000,000). Beijing: Geological Publishing Housea.

Villaseñor, A., M. H. Ritzwoller, A. L. Levshin, M. P. Barmin, E. R. Engdahl, W. Spakman, and J. Trampert (2001). Shear velocity structure of central Eurasia from inversion of surface wave velocities, *Phys. Earth Planet. Int.* 123: 169–184.

Vinnik, L. P., S. W. Roecker, G. L. Kosarev, S. I. Oreshin, and I. Y. Koulakov (2002a). Crustal structure and dynamics of the Tien Shan, *Geophys. Res. Lett*. 29: 2047, doi: 10.1029/2002GL015531.

Vinnik, L. P., D. Peregoudov, L. Makeyeva, and S. Oreshin (2002b,).Towards 3-D fabric in the continental lithosphere and astenosphere: The Tien Shan, *Geophys. Res. Lett.* 29: 1795, 10.1029/2001GL014588.

Vinnik, L. P., C. Reigber, I. M. Aleshin, G. L. Koserev, M. K. Kaban, S. I. Oreshin, and S. W. Roecker (2004). Receiver function tomography of the central Tien Shan, *Earth Planet. Sci. Lett*. 225: 131–146.

Wang, Q., et al. (2001). Present-day crustal deformation in China constrained by global positioning system measurements, *Science* 294: 574–577.

Watson, M. P., A. B. Hayward, D. N. Parkinson, and Z. Zhang (1987). Plate tectonic history, basic development and petroleum source rock deposition of onshore China, *J. Mar. Petr. Geol*. 4: 205–225.

Wittlinger, G., J. Vergne, P. Tapponnier, V. Farra, G. Poupinet, M. Jiang, H. Su, G. Herquel, A. Paul (2004). Teleseismic imaging of the subducting lithosphere and Moho offsets beneath western Tibet, *Earth Planet. Sci. Lett*. 221: 117–130.

Yin, A., S. Nie, P. Craig, M. T. Harrison, F. J. Ryerson, Q. Xianglin, and Y. Geng (1998). Late Cenozoic tectonic evolution of the southern Chinese Tien Shan, *Tectonics* 17: 1–27.

Zhao, J., G. Liu, Z. Lu, X. Zhang, and G. Zhao (2003). Lithosperic structure and dynamic processes of the Tian Shan orogenic belt and the Junggar basin, *Tectonophys.* 376: 199–239.

Zhao, J., H, Liu, S. Pei, S. Jia, B. Liu, J. Zhang, and J. Fan (2006). A geophysical transect of the lithosphere across the eastern Tienshan orojen, (submitted).

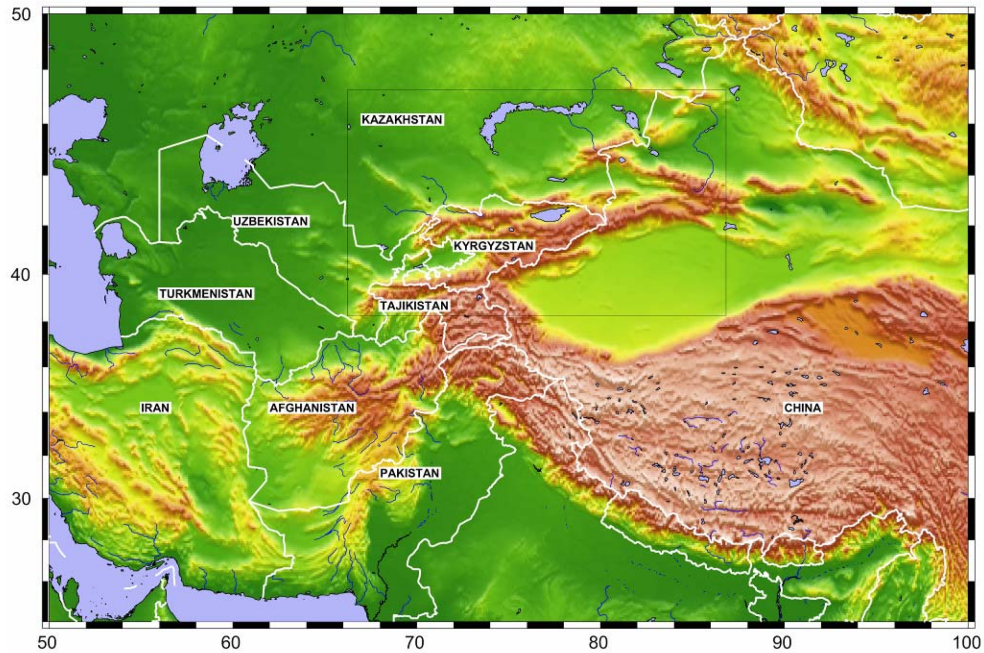

Figure 1. CASRI project area political boundaries and topography.

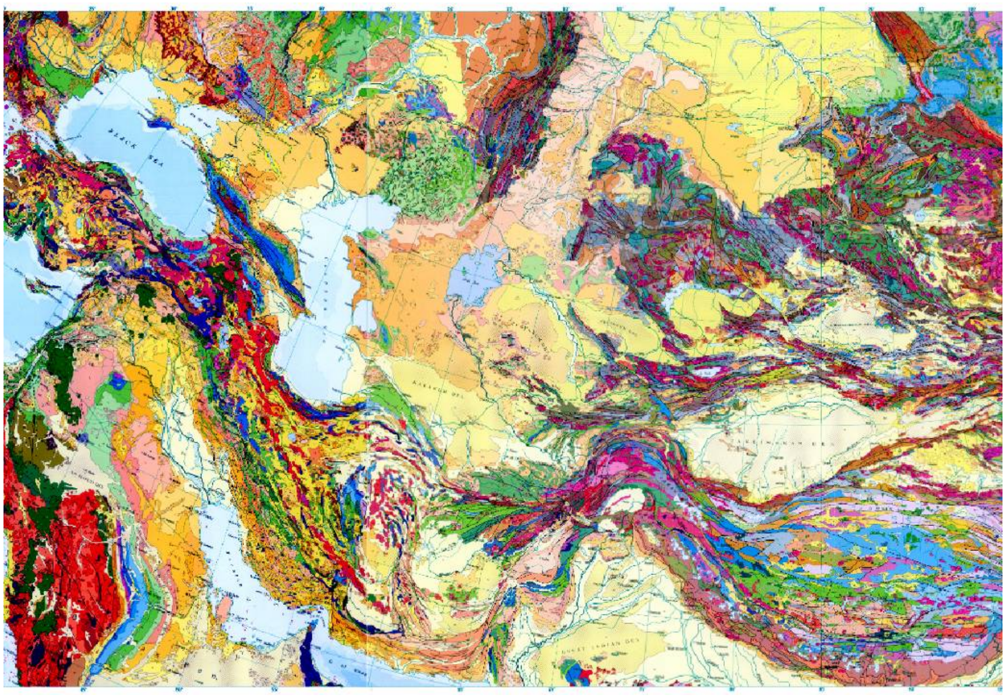

Figure 2. Geological map compilation of the CauSIN and CASRI regions.

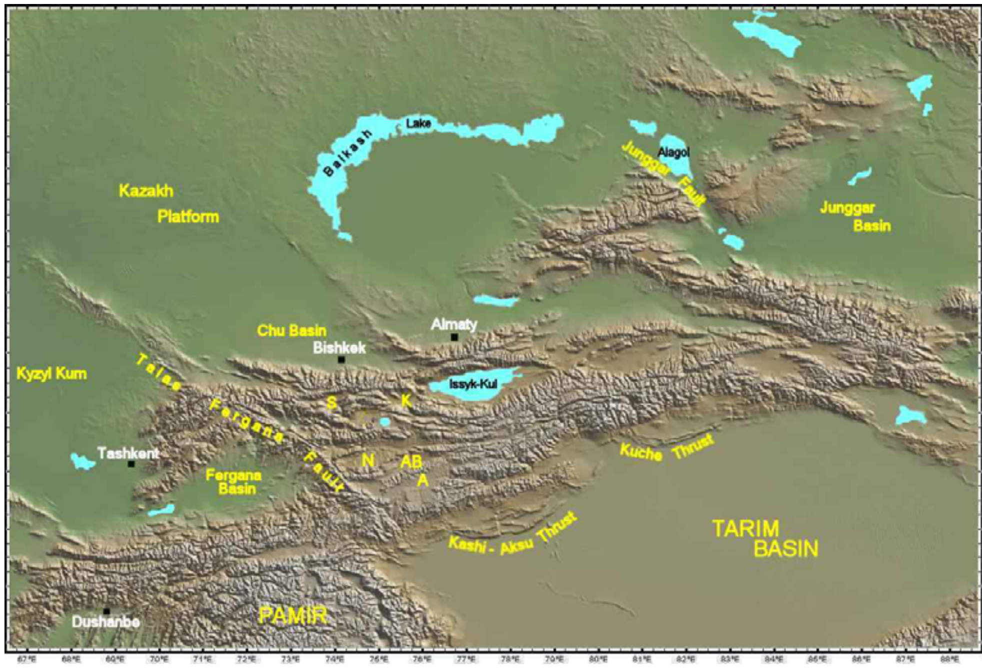

Figure 3. Shuttle Radar Topographic Mission (SRTM) image showing tectonics and topography of the Tien Shan and surrounding regions. The east-west trending lineaments are the active thrust faults in the Tien Shan. Basins are S, Suusamyr; K, Kochkor; N, Naryn; AB, At-Bashi; and A, Aksay.

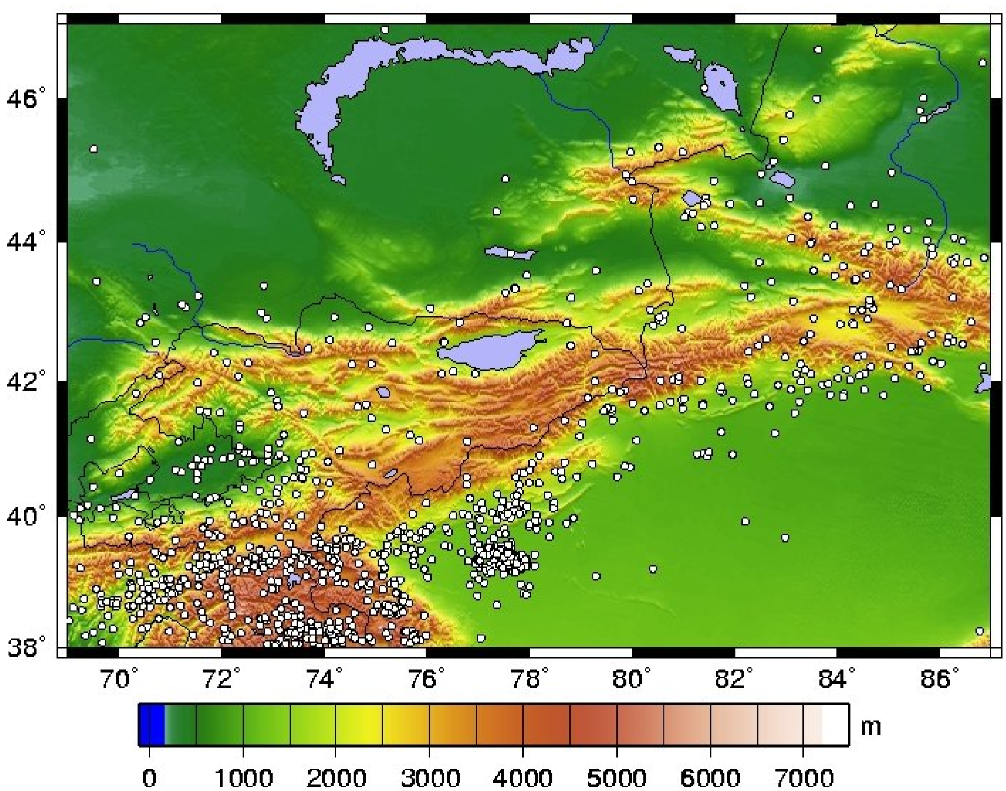

Figure 4. Seismicity map of the Tien Shan and surrounding regions. The seismicity data cover the events with M>4 for the period 2000-2004 from the ISC Comprehensive database.

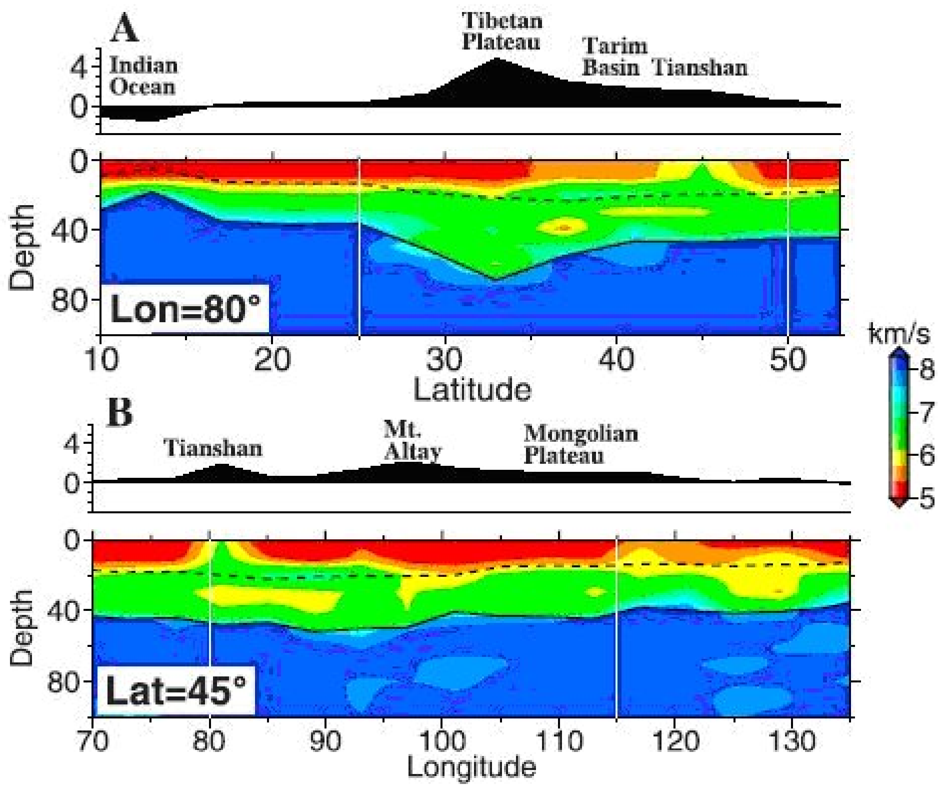

Figure 5. Cross sections showing P-wave velocity variations along N-S (A) and E–W (B) directions beneath central Asia (Sun and Toksöz, 2006). The dashed lines indicate the Conrad discontinuity.